Overview

Understanding the dynamics behind photoisomerization of light-driven molecular rotary motors

Michael Filatov*

The design and synthesis of artificial molecular motors to power up the nanoscale mechanical devices is one of the urgent tasks for modern synthetic chemistry. Light-driven molecular rotary motors are a key class of compounds that undergo unidirectional rotation about a double bond through a series of photochemical and thermal steps. To improve their functionality and to develop new design strategies, a deeper understanding of the dynamics behind light-driven rotary motion is required. Such an understanding can be only gained from the accurate dynamics simulations of the nonadiabatic photo-rearrangement processes occurring during the motor operation. The currently available methods of quantum chemistry combined with the nonadiabatic molecular dynamics techniques represent a powerful tool for the investigation of the dynamic aspects of the molecular motors functionality. The results obtained in theoretical simulations provide for an unprecedented understanding of the photoisomerization process and hold considerable implications in achieving improved design strategies for future generations of molecular motors.

How to cite this article:
WIREs Comput Mol Sci 2013, 3: 427–437 doi: 10.1002/wcms.1135

INTRODUCTION

Nature has ingeniously designed molecular motors, which play a central role in biology as the means of movement in living organisms. Chemistry is at an early stage of building artificial molecular motors at the bench.[1–3] Currently, there is a high interest within the synthetic chemistry community in developing molecular motors and applying them in nanoscale mechanical devices.[4–6] Various types of molecular motors have been synthesized, which can use different sorts of energy input. In this regard, one can distinguish chemically driven,[7,8] electrochemically driven,[9,10] and light-driven molecular motors.[11–13] The latter type of motors seems to be the best suited for many practical applications as they can achieve continuous unidirectional rotary motion without producing waste products, which may impair their function.[4,14] Indeed, light-driven molecular rotary motors already find application in engineering functionalized surfaces[15] (e.g., for transporting liquids and macroscopic objects) and in building nanocars.[9,16,17]

Rational synthetic design of light-driven molecular rotary motors, however, implies a thorough understanding of their functionality. The thermochemical aspects of their operation are well understood, whereby empirical studies and judicious chemical modification have allowed for a very high degree of control over the thermal step limited rotation speed and a considerable gain in the speed (ca. 10^8 times) has been achieved by lowering the thermal helix inversion barrier.[11–13,18] Their photodynamics however still remains obscure and less amenable to judicious chemical modification. To be able to improve the design of light-driven molecular rotary motors, one needs to better understand the underlying mechanism

*Correspondence to: mike.filatov@gmail.com
Mulliken Center for Theoretical Chemistry, Institut für Physikalische und Theoretische Chemie, Universität Bonn, Bonn, Germany
DOI: 10.1002/wcms.1135

and the effect of various factors, such as substituents, heteroatoms, and environment, on the dynamics of photo-rearrangement. Such knowledge will have far-reaching implications for achieving a rational synthetic design of future molecular photo-driven systems and will help to improve their functionality. This is a key to their application in future molecular devices in nanotechnology and synthetic biology.

The accurate and reliable modeling of photoreactions represents a considerable challenge for the contemporary chemical theory as these processes typically occur on (sub-)picosecond and even femtosecond time scale and they are far from equilibrium. The nonequilibrium nature of these processes renders the traditional approaches to describing reaction rates and reaction pathways highly unreliable for determining mechanism of photoreactions and necessitates the use of molecular dynamics methods, in which the nuclear dynamics problem is solved simultaneously with the (multistate) electronic structure problem. This necessity puts an additional strain upon the electronic structure theory as it requires the accurate and balanced description of dynamic and nondynamic electron correlation effects arising in the ground and excited electronic states of large molecules.[19,20] Stemming from these difficulties, there is only a limited number of theoretical investigations of the photodynamics of light-driven molecular rotary motors available in the literature.[21–24] Notwithstanding the scarcity of publications on the topic, it seems worthwhile to provide a concise overview of the major results obtained so far as regards the theoretical modeling of the photodynamics of molecular motors and their implications for achieving a rational synthetic design of future molecular motors with application defined functionality.

SYNTHETIC LIGHT-DRIVEN MOLECULAR ROTARY MOTORS

Light-driven molecular rotary motors derived from chiral overcrowded alkenes represent a central class of compounds for which photochemical rearrangements play a crucial role in their function.[11–14] The mode of action of these motors is based on the periodic repetition of photoisomerization and thermal relaxation steps, which lead to a unidirectional rotation of one part of the molecule (rotor) with respect to another (stator). Scheme 1 shows the operation cycle of a typical rotary molecular motor, 9-(2,4,7-trimethyl-2,3-dihydro-1H-inden-1-ylidene)-9H-fluorene.[13] It is this motor that finds application in designing functionalized surfaces[15] and in building nanocars, which were able to travel substantial distances on a solid surface.[9]

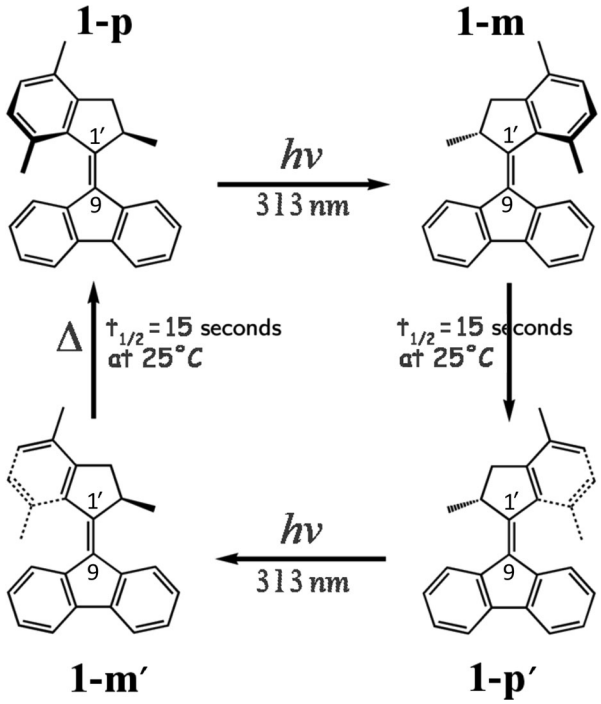

SCHEME 1 | Operation cycle of molecular motor **1**.

In the operation cycle of the rotary motor **1**, the photoisomerization step (power stroke), which occurs on a picosecond time scale,[13,25] brings the molecule from its stable conformation, **1-p**, to a metastable conformation, **1-m**, which then relaxes to another stable conformer **1-p′** via thermally activated helix inversion pathway. The latter process is the rate-limiting step of the operation cycle of the motor. The whole operation cycle has an overwhelming preference for one sense of rotation as a consequence of the relative thermodynamic stability of the **1-p** and **1-m** conformers (**1-p** is more stable by 3.5 kcal/mol)[13,23,24] and the quantum yields of the photoisomerization reactions. In the photostationary state (PSS) of **1** observed experimentally at a wavelength of 365 nm, the ratio of the concentrations of the **1-p** conformer to the **1-m** conformer is 1:3 (with ca. 10% SD).[13] This suggests that the quantum yield of the forward isomerization **1-p** → **1-m** is greater than the quantum yield of the inverse photoreaction **1-m** → **1-p**. As the absorption spectra of the two conformers have a substantial overlap at the excitation wavelength,[13] the strong preference for one conformer suggests that **1-p** and **1-m** undergo different isomerization pathways in the excited state.

Over several generations of rotary molecular motors, a considerable increase in the rotation

speed (ca. 10^8 times) has been achieved by synthetic chemistry means—by introducing various substituents and redesigning the shape of the stator and the rotor blades—due to lowering the thermal helix inversion barrier.[11–13,18] Ideally, a similar degree of control should be achieved over the photoisomerization step to make molecular motors better suited for specific applications in molecular machines and devices. It should be emphasized that all usable rotational work is performed during the photoisomerization step, whereas in the helix inversion step, the motor is idling by resetting itself to a conformation suitable for further operation. However, quite little is known about the dependence of the parameters of the photoreaction (power stroke) on the geometric structure of the motor, substituents, and heteroatoms introduced into the rotor and the stator units, and interactions with the environment and/or substrate on which the motor is anchored. For instance, it has been established experimentally that introducing substituents in motor **2** (X = —O—Me, —CN, —H) results in very different photoequilibria ranging from 53:47 to 82:18.[26] Such a wide variation in the PSS ratio cannot be explained without a detailed and thorough investigation of the dynamics of the pertinent photoreactions. This is especially true in view of the fact that the motor molecule undergoes an ultra-fast and barrierless isomerization on the excited-state surface,[25] which implies that the statistical theories of reaction rates, such as the transition state (TS) theory, are unlikely to provide a sensible description of these processes. It is therefore essential to apply the methods of nonadiabatic quantum or semi-classical dynamics to investigate the mechanism of photoisomerization of molecular motors in relation to their molecular structure.

THEORETICAL MODELING OF PHOTOCHEMISTRY

During the last decades, understanding of the photochemistry underwent a gradual transition from a zero-dimensional picture, in which molecular transformations in the excited states and radiationless relaxation to the ground state were analyzed solely in terms of Fermi's golden rule and the Franck–Condon principle, to a one-dimensional picture, where molecular transformations in the excited state were described in terms of a specific reaction coordinate (e.g., twist about the double C=C bond), and radiationless relaxation was assumed to occur in the avoided crossing region, to a multidimensional picture, in which the molecular transformations and radiationless relaxation processes occur primarily via conical intersection (CI) points or seams.[27] With the advent of ultra-fast optical spectroscopic methods,[28] it became clear that the excited states of molecules undergo the transformation and radiationless relaxation to the ground state too fast to be described in terms of the nonadiabatic coupling in the avoided crossing regions alone. Since the pioneering works of Yarkony[29] and Robb and coworkers,[30] the role of CIs in molecular photochemistry and for predicting the direction of molecular photo-rearrangements has been recognized. A clear example is the understanding of the photochemistry of small organic alkenes, such as ethylene, for which pyramidalization of one of the carbon atoms plays (along with the twist about the double C=C bond) a crucial role in the course of the photo-rearrangement.[27,31,32]

The Born–Oppenheimer approximation (BOA)[33] is the central concept in chemical theory, which enables one to describe chemical reactions as (quasi-)classical processes occurring on well-separated and sharply defined potential energy surfaces (PESs). In photochemical reactions, the breakdown of BOA is the rule rather than exception, as one needs to include into consideration a possibility of nonadiabatic radiationless transitions between different PESs, for instance the π-π^* excited electronic state of C=C bond and its ground electronic state. For these transitions, CIs, being the most efficient channels of radiationless population transfer between the electronic states, play a role similar to the TSs of thermally activated chemical reactions.[27,29,30,34] CIs however are multidimensional manifolds of points of true crossing between the PESs. Because of the noncrossing rule for the electronic states of the same spin and space symmetry,[35–37] true crossings between PESs may occur only in the space of at least two dimensions. Generally, crossing between two N dimensional PESs, for example, I and J electronic states, may occur in the space of N-2 dimensions, the CI seam. The CI seam can be best characterized in the space of two collective displacements, the nonadiabatic coupling vector $\vec{f}_{IJ}$ and the difference gradient $\vec{g}_{IJ}$, along which the degeneracy of the electronic states is lifted linearly.[29]

The breakdown of the BOA near the CI seams manifests itself in the divergent nonadiabatic coupling vector, Eq. (1),

$$\vec{f}_{IJ} = \left\langle \Psi_I \left| \frac{\partial}{\partial \vec{R}} \right| \Psi_J \right\rangle = (E_J - E_I)^{-1} \times \left\langle \Psi_I \left| \frac{\partial \hat{H}^{\mathrm{el}}}{\partial \vec{R}} \right| \Psi_J \right\rangle = (E_J - E_I)^{-1} \vec{h}_{IJ} \quad (1)$$

where $\vec{R}$ is the vector of nuclear coordinates, $\hat{H}^{el}$ is the electronic Hamiltonian (in the BOA), and Ψ_X and $E_X(X = I, J)$ are its eigenfunctions and eigenvalues. When multiplied by the nuclear momentum operator, the nonadiabatic coupling vector yields the off-diagonal part of the nuclear kinetic energy operator that promotes transitions between the adiabatic electronic states.[29] Thus, the probability of the nonadiabatic transitions between the electronic states is dominated by the geometries in the vicinity of the CI seam.

As the CI seams are multidimensional manifolds, they are often characterized by local minima along the seam, the minimal energy CIs (MECIs). A variety of computational techniques can be used to locate the MECIs,[31,38,39] which were applied to characterize the nonadiabatic relaxation processes in many photoreactions, including the paradigmatic systems such as ethylene,[40,41] protonated Schiff base,[42] stilbene,[41] and so on.[27,31] To a certain extent, the use of MECIs for deducing the pathways of photoreactions is similar to the use of the intrinsic reaction coordinate approach[43] to the ground-state thermally activated reactions. However, because of their ultrafast nature, photoreactions may not necessarily occur through MECIs and other parts of the CI seam may play a more significant role.[27,32,44] Besides the local topography of the CI points, where peaked and sloped CIs can be distinguished, with the former providing for more efficient funnels of the population transfer,[45] the proximity to the Franck–Condon region on the excited-state PES (minimal distance CI, MDCI)[31] may also be important for the involvement of different parts of the CI seam in the radiationless relaxation process. Although conceptually MECIs, MDCIs and their topography are important descriptors of the crossing seams, the ultimate answer to their relevance for the dynamics of the given photoprocess can be only given by molecular dynamics simulations.[27,32]

Nonadiabatic Molecular Dynamics

Since the seminal work of Car and Parrinello,[46] *ab initio* molecular dynamics (AIMD) has become a powerful tool for explaining time-dependent properties of chemical systems. Rooted in the BOA, AIMD meets two primary challenges, when describing nonadiabatic dynamics of photo-reactions: (1) the necessity to accurately describe the ground and excited electronic states of molecules far from the equilibrium geometry, and (2) the necessity to include the quantum effects into the dynamics, which allow for the transfer of energy between the electronic and nuclear degrees of freedom and thereby for the nonadiabatic transitions. The former requirement implies that the quantum mechanical methods used to obtain the electronic states have to provide for a balanced treatment of both the dynamic as well as the nondynamic electron correlation effects, which become important for molecules with broken or distorted chemical bonds. As the quantum mechanical electronic structure problem is solved simultaneously with the classical equations of nuclear dynamics, the proper description of the feedback between quantum and classical degrees of freedom becomes crucial.

Within the paradigm of mixed quantum-classical (MQC) dynamics, the self-consistent description of the quantum-classical feedback is achieved with the use of two general approaches: the Ehrenfest method[47,48] and the trajectory surface hopping (TSH) method.[49,50] Both computational approaches are capable of describing quantum transitions driven by nuclear motion, properly conserving the total—that is quantum plus classical—energy, and including quantum coherence effects. In the Ehrenfest method, the classical force field acting on the nuclei is derived from the weighted average of several electronic state PESs (mean-field approximation), with the time-dependent weights obtained by integration of a semi-classical time-dependent Schrödinger equation (SC-TDSE).[51] The major drawbacks of the Ehrenfest method stem from the use of the mean-field force to propagate a single classical trajectory for nuclei. When living a region of strong nonadiabatic coupling, the single trajectory still evolves on a mean-field PES, although the physics requests it to remain on one surface.[50] Ultimately, this may lead to an incorrect dynamics especially for the case of PESs separated by a large amount of energy.[50] Finally, in the long time limit, the Ehrenfest method leads to a much too high energy of the quantum subsystem and to non-Boltzmann population of the electronic states.[52]

The TSH approach is free of these drawbacks and has been shown to be more accurate than the Ehrenfest method in many MQC applications.[52] In the TSH approach, the classical force that drives the nuclear dynamics is derived from the PES of a single electronic state, not a mean-field force. The electronic state can switch at any point along the trajectory as governed by a stochastic hopping algorithm.[50] The quantum-classical feedback is achieved by a total-energy-conserving change of the nuclear momentum in the direction of the nonadiabatic coupling vector, Eq. (1), when the transition between the electronic states occurs. Typically, a swarm of trajectories is propagated and the hopping between PESs is done in such a way that it maintains consistency between

the fraction of trajectories evolving on a particular PES and the population of that electronic state as given by the integration of the SC-TDSE.[50,51] The most common algorithm for deciding whether to hop or to stay on the same PES is the fewest switches method,[50] which minimizes the number of hopping events within the time increment Δt used for the integration of the classical equations of motion. Perhaps the most significant advantage of the TSH method with the fewest switches algorithm is that it obeys the detailed balance condition and yields correct Boltzmann populations of the electronic states in the long time limit. Furthermore, the TSH method is capable of correctly describing branching of trajectories when passing through a region of strong nonadiabatic coupling between PESs.[50] Because of these advantages, the TSH method appears to be the method of choice for modeling the nonadiabatic dynamics, especially the photodynamics.[51] For further details of the TSH method and its applications, the reader is referred to a review article by Barbatti.[51]

Besides the discussed MQC dynamics methods, a number of more accurate algorithms for modeling the nonadiabatic dynamics are available. The numerically exact wave-packet propagation schemes, such as the multiconfiguration time-dependent Hartree method,[53] provide for an accurate account of the quantum character of nuclear motion. However, the computational cost of these methods for large molecules, such as the molecular motors, is prohibitively high. The full multiple spawning[54] and *ab initio* multiple spawning[55] methods occupy an intermediate place between the wave-packet propagation methods and MQC dynamics approaches. Although these approaches have been successfully applied to modeling the nonadiabatic dynamics of several relatively small-molecular systems,[27,31,40,41] their computational cost remains sufficiently high and, for large molecules, the MQC methods are preferred.

Quantum Chemical Methods for Nonadiabatic Molecular Dynamics

The methods of electronic structure theory used in connection with modeling of the nonadiabatic dynamics of photoreactions have to satisfy a number of requirements, the most important of which is their (a) ability to provide for a balanced and accurate description of the dynamic and nondynamic electron correlation effects in the ground and in the excited electronic states of large molecules. A very desirable feature is (b) the availability of the analytic energy gradients for the ground and excited states and the analytic nonadiabatic coupling vectors, Eq. (1). Furthermore, to allow for an on-the-fly quantum calculations during the dynamics runs, (c) the computation cost should be sufficiently low.

The criterion (a) is satisfied by the multireference methods of wavefunction quantum chemistry, such as the complete active space self-consistent field (CASSCF) method with the second-order many-body correlation correction (CASPT2)[20,22] and the multireference configuration interaction with single and double excitations [MR(S)-DCI].[22] Although the analytic energy gradient is available for some variants of the CASPT2 method[56,57] and for the MR(S)-DCI method,[58,59] the computational cost for molecules as large as molecular motors is prohibitively high. The CASSCF method has lower computation cost; however, it misses the dynamic electron correlation and, as a consequence, is not capable of accurately describing the PESs of the electronic states.

The methods of Kohn–Sham density functional theory (KS-DFT)[60] enjoy a great success among computational chemists, primarily due to their low computation cost and the fact that the electron correlation (dynamic and a part of nondynamic)[61] is approximately included in the calculations via the use of density functionals. In the context of KS-DFT, the excited states can be accessed via the use of time-dependent DFT (TD-DFT),[62] which provides for the excitation energies sufficiently accurate for many spectroscopic applications. In its standard form, however, KS-DFT is not capable of accurately describing the nondynamic electron correlation and, consequently, the TD-DFT method breaks down for the situations where strong nondynamic correlation is present in the ground electronic state.[63] As avoided crossings and true crossings (CIs) of the ground and excited states cannot be reliably described with the use of the standard KS-DFT methods, one needs to develop alternative cost-efficient approaches in the domain of DFT.

A computational scheme based on the ensemble approach to DFT[64] has been recently implemented in the form of the spin-restricted open-shell KS (ROKS) method[65] and the spin-restricted ensemble-referenced KS (REKS) method.[66] In these methods, the nondynamic electron correlation is taken into account via the use of the fractional occupation numbers of the active KS orbitals and the representation of the total energy and the density of a strongly correlated system in the form of weighted sums (ensembles) of the individual KS configurations. In the REKS method, the weighting factors are variationally optimized together with the KS orbitals, whereas they are kept fixed in the ROKS method, in which only the KS orbitals are optimized. The REKS method is capable of accurately

describing the ground-state PES of molecules with completely or partially broken bonds, such as molecular motors undergoing photoisomerization. Certain states of the open-shell singlet character, such as the π-π^* excited state of C=C bond, can be accessed with the use of the ROKS method[67]; however, a direct application of DFT to the optimization of the excited-state energy and density is prohibited on the formal grounds[68] and may lead to artifacts.[69] This difficulty is remedied in the state-averaged REKS (SA-REKS) method, in which a weighted sum of the ground-state REKS energy and the excited-state ROKS energy is variationally optimized in compliance with the rigorous theory.[68] Hence, the SA-REKS method represents a cost-efficient alternative to the high-level multireference methods of wavefunction quantum chemistry. Although the SA-REKS method gives access to the accurate ground and excited-states PESs of molecular motors undergoing photoisomerization, presently, the analytic energy gradient for the excited state and the nonadiabatic coupling vector calculation are not yet implemented and this impedes an efficient use of this approach for on-the-fly calculation during the TSH nonadiabatic dynamics simulations.

A considerable speed up in the calculation of the electronic states is achieved with the use of semiempirical quantum chemical methods. In particular, the orthogonalization-corrected method (OM2),[70] in connection with the graphical unitary group approach to multireference configuration interaction (GUGA-MRCI)[71] as implemented in the MNDO suite of programs,[72] is capable of providing sufficiently accurate information on the ground and excited states of large molecules at a very low computational cost. The OM2/GUGA-MRCI method can be directly used for on-the-fly calculation of the electronic states in connection with the TSH nonadiabatic dynamics formalism and is capable of yielding sufficiently accurate description of the nonadiabatic dynamics.[73]

DYNAMICS OF PHOTO-REARRANGEMENT OF MOLECULAR MOTORS

The first synthetic light-driven rotary molecular motor, (3R,3′R)-(P,P)-trans-1,1′,2,2′,3,3′,4,4′-octahydro-3,3′-dimethyl-4,4′-biphenanthrylidene, **3**, for which a unidirectional rotary motion has been experimentally verified,[11] was a subject of probably the first nonadiabatic dynamics investigation by Grimm et al.[21] The working cycle of the motor **3** is similar to that shown in Scheme 1 and the first photoisomerization step leading from the stable conformer, (P,P)-trans-**3**, to a metastable conformer, (M,M)-cis-**3**, has been simulated using the Car–Parrinello molecular dynamics where the ground S_0 electronic state was calculated using the KS/BLYP method and the ROKS/BLYP method was used for the lowest open-shell singlet excited S_1 state (π-π^* excitation around the C_4=$C_{4'}$ bond). It was found that, after the photoexcitation to S_1, within a time shorter than 1 picoseconds the (P,P)-trans-**3** conformer undergoes a quick rotation about the C_4=$C_{4'}$ bond toward the 90° of twist where the excited S_1 PES crosses the S_0 PES and a nonadiabatic population transfer occurs.[21] There was no indication that, at the crossing point, pyramidalization of the carbon atoms at the central C_4=$C_{4'}$ bond takes place.

Given the criticism of the use of the ROKS approach alone for the calculation of the excited-state PES, it is not surprising that the results obtained in Ref 21 are highly unreliable. The S_1 state lifetime (ca. 0.8–1 picoseconds) is much too short in comparison with the lifetimes measured experimentally for similar molecular motors (ca. 1.5–1.7 picoseconds).[25,74] Furthermore, in a homopolar molecule, such as **3**, at 90° of twist not accompanied by pyramidalization an avoided crossing of the S_1 and S_0 PESs should occur rather than a true crossing. This was indeed confirmed by Kazaryan and Filatov,[22] who found, using the SA-REKS method for the same motor **3**, that an avoided crossing is present at 90° of twist with the energy gap of ca. 1.7 eV. Indeed, the approach employed in Ref 21 is not capable of properly describing complete or partial bond dissociation in the ground state and avoided crossings between the ground and excited states.

The first reliable modeling of the nonadiabatic dynamics of molecular motor **1** has been carried out by Kazaryan et al.[23] with the use of the SA-REKS calculations and molecular dynamics simulations. Using SA-REKS and TD-DFT calculations in connection with the BH&HLYP density functional, it was found that, at the equilibrium geometries of the **1-p** and **1-m** conformers, the lowest excited S_1 state corresponds to the π–π^* excitation of the central C_9=$C_{1'}$ bond (see Scheme 1). The S_1 state has a zwitterionic character, is optically accessible, and it leads to breaking the π-component of the C_9=$C_{1'}$ bond. This state is therefore photochemically active and, as shown in Figure 1, the S_1 PES features a substantial slope from the FC point toward twisted-pyramidalized structure near which CI seam is met.[23] The S_0 and S_1 PESs shown in Figure 1 were obtained by scanning the electronic energies of the respective states on a rectangular grid spanning the twisting angle θ and the pyramidalization angle α (see inset in Figure 1). As the scans are

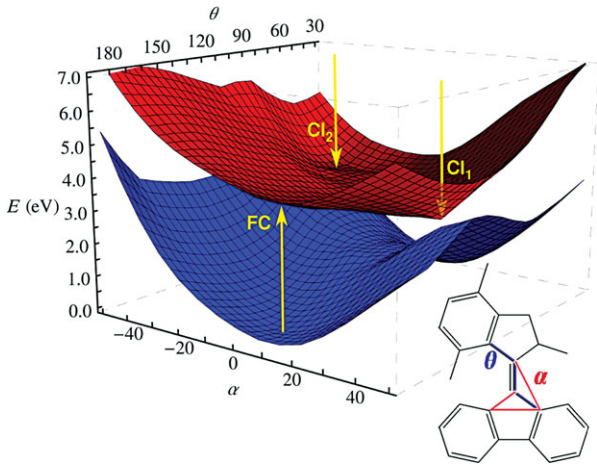

FIGURE 1 | Profiles of the S_0 (blue) and S_1 (red) potential energy surfaces of the molecular motor **1** obtained in the SA-REBH&HLYP/6-31G* calculations. Positions of the Franck–Condon points and conical intersections are shown with arrows. The inset shows definitions of the twist angle θ and pyramidalization angle α. (Adapted with permission from Ref 23. Copyright 2012, American Chemical Society.)

carried out in a 2D space, the CI seam manifests itself as two CI points, CI_1 and CI_2, of which the former lies closer to the FC point of **1-p** conformer and the latter to the FC point of **1-m** conformer.

According to the SA-REKS/6-311+G** calculations, the CI_1 point lies 0.7 eV below the **1-p** FC point (calc.: 3.71 eV, exp.: 3.44 eV[13]) and the CI_2 point is 0.5 eV below the **1-m** FC point (calc.: 3.31 eV, exp.: 3.22 eV[13]). There is therefore a substantial energy gradient from the FC points toward the CI seam; however, to reach the CIs, the motor **1** should undergo not only a twist about C=C bond, but a simultaneous pyramidalization of the C_9 atom. Pure twist not accompanied by the pyramidalization leads to an avoided crossing region seen in Figure 1. As both CIs have peaked topography, they can serve as very efficient funnels of population transfer from the S_1 to the S_0 PES.[23]

At the time of writing Ref 23, the analytic gradients and nonadiabatic coupling vectors for the excited state were not implemented for the SA-REKS method, and the molecular dynamics simulations were carried out using classical force fields. In these simulations, a specially parametrized all-atom OPLS force field was employed, which reproduced the shape and the major features on the S_1 and S_0 PESs obtained with SA-REKS. Proximity to the obtained CI_1 and CI_2 points was used as a criterion for the surface hop; The molecular dynamics runs were initiated on the S_1 PES, starting from a geometry randomly selected from a ground-state equilibration run, and the trajectory evolved on that PES until (and if) it reached a geometry within a predefined RMSD threshold from either of the CIs. Upon reaching the CI, a momentum-conserving surface hop was initiated and the trajectory continued on the S_0 PES.[23] Analysis of the obtained trajectories revealed that the motor performs a strongly damped twist about the C_9=$C_{1'}$ bond coupled with a weaker damped pyramidalization of the C_9 atom vibrational motion. Within less than 0.5 picoseconds, the motor reaches nearly 90° of twist and performs 1–2 pyramidalization vibrational cycles before reaching a geometry in the vicinity of the CI seam (see Figure 5 in Ref 23).

Although these molecular dynamics simulations were based on an *ad hoc* assumption regarding the nonadiabatic population transfer (hops at the CIs only), they produced fairly reasonable predictions for the S_1 state lifetimes and for the quantum yields of photoisomerization. Thus, the lifetime of the S_1 state was predicted to be 1.40 ± 0.10 picoseconds when starting from the **1-p** conformer and 1.77 ± 0.13 picoseconds when staring from the **1-m** conformer.[23] The ratio of the quantum yields of the **1-p** → **1-m** and the **1-m** → **1-p** photoisomerizations corrected for the overlap of absorption spectra yielded 1:3.5 for the PSS ratio of the concentrations of the **1-p** and **1-m** conformers,[23] in an excellent agreement with the experimentally obtained 1:3 ratio.[13]

It was thus established computationally that the motor **1** has a preference for one sense of rotation, as shown in Figure 2. This preference is the consequence of a preferred direction of photoisomerization, **1-p** → **1-m**, as manifested in the quantum yields, and a preferred direction of thermal helix inversion, as determined by the relative stability of the **1-p** and **1-m** conformers. During its operation cycle, motor **1** undergoes a strong twist-pyramidalization motion and its photoisomerization mechanism is, in a general sense, similar to the mechanism of ethylene photoisomerization.[27,41] The large-scale motion performed by the motor (see Figure 2) is not a pure rotation about the central C=C bond, which holds considerable implications for developing design strategies for future generations of molecular motors.

The conclusions of Ref 23 have been later confirmed and extended by more rigorous TSH nonadiabatic molecular dynamics simulations by Kazaryan et al.,[24] in which the semi-empirical OM2/GUGA-MRCI Hamiltonian was used to obtain the electronic states of molecular motor **1**. Analysis of the S_0 and S_1 PESs of **1** obtained in these calculations revealed the shape of the CI seam, on which no low energy geometries not featuring pyramidalization were found.

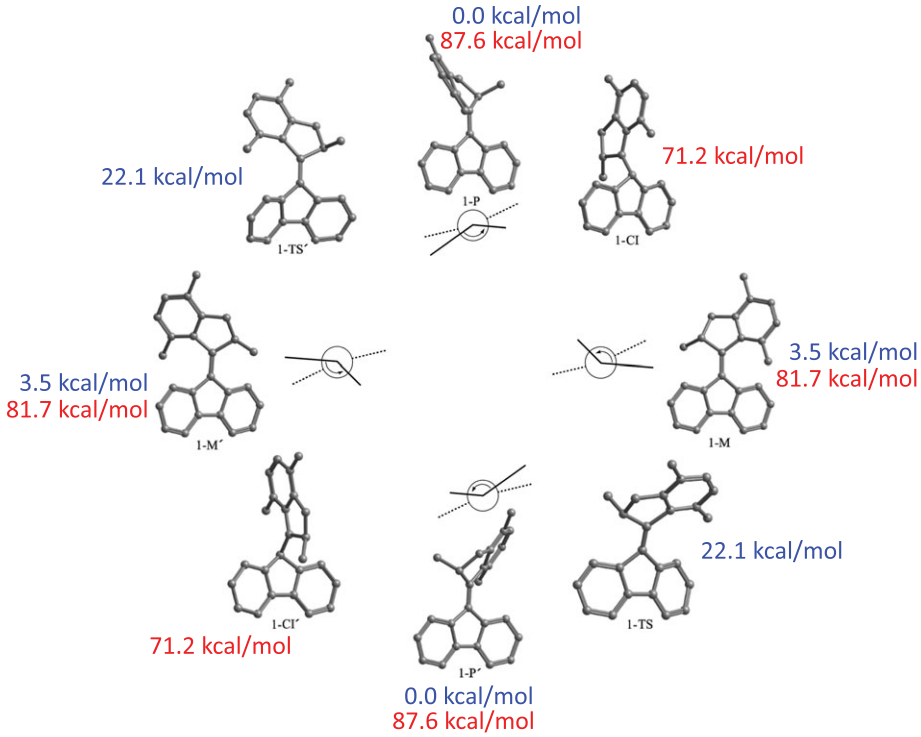

FIGURE 2 | Geometries of the most important structures involved in the rotation cycle of molecular motor **1** as obtained from the SA-REBH&HLYP/6-31G* calculations. Hydrogen atoms were removed for clarity. The relative energies for the ground-state structures (blue) and for the excited-state structures (red) obtained with the SA-REBH&HLYP/6-31G* method are given. (Adapted with permission from Ref 23. Copyright 2012, American Chemical Society.)

The TSH-OM2 simulations yielded the S_1 lifetimes of 1.4 picoseconds (**1-p**) and 1.79 picoseconds (**1-m**) and the PSS ratio (**1-p/1-m**) of 1:2.7 in an excellent agreement with the previous calculations. Furthermore, analysis of the TSH-OM2 trajectories revealed that the population transfer occurs via the CI seam and that the avoided crossing region does not play a role for the photoisomerization, in this way corroborating the assumptions in Ref 23. A more detailed analysis of the trajectories pointed out that the surface hops occur not necessarily at the MECIs and other parts of the CI seam are involved in the nonadiabatic transition. This finding is in a general accord with the analysis of the AIMS simulations for photoisomerization of small organic molecules.[27,31,32]

At the time of writing of Refs 23 and 24, no experimental data regarding the excited-state lifetimes of **1** nor a mechanism underlying the photoisomerization were available. Such data emerged only recently, in Ref 25, where ultra-fast fluorescence upconversion measurements and transient absorption measurements on the power stroke of molecular motor **2-H**, closely related to **1**, were undertaken. According to the experiential data of Conyard et al.,[25] the photoisomerization occurs via CIs between the S_1 and S_0 states and the measured S_1 lifetime is 1.5 ± 0.3 picoseconds, in an excellent agreement with the theoretical predictions. A very fast initial motion that leads the motor away from the FC point was detected in the ultrafast fluorescence upconversion experiments,[25] which is in agreement with the theoretical analysis of the trajectories obtained in Ref 23. Furthermore, the measured difference of the quantum yields of the direct and the inverse photoisomerization reactions is 0.14 in an excellent agreement with the theoretical difference of 0.16 (see Figure 8 in Ref 24), thus, fully confirming the mechanism predicted from the theoretical simulations.[23,24]

CONCLUSIONS

In the quest for more efficient and more powerful molecular motors, one needs to gain control over all the aspects of their functionality. In particular, the photoisomerization step (see Scheme 1) requires a special attention, as currently there are no concise empirical prescriptions that would enable one to tweak the parameters of the photoreaction, such as the PSS ratio, excited-state lifetimes, and sequence of the

geometric changes that a molecule undergoes on the exited state PES, at will. Currently, such knowledge can be reliably obtained using a combination of modern quantum chemical methods, such as those discussed in the present overview, with the TSH nonadiabatic molecular dynamics simulations. Although modeling of the molecular motor operation cycle is a relatively new, emerging field of theoretical research, the results obtained so far shed a light on the mechanism behind the photoisomerization of molecular motors, the role of CIs and geometric changes necessary to reach them. The future research will address the theoretical study of substituent effects and heteroatom effects on the profiles of the ground and excited-state PESs, on the occurrence and position of CI seams and on the nonadiabatic couplings between the PESs. Understanding these factors as well as the interactions with the environment will provide information necessary for designing new molecular motors with improved capabilities for practical applications.

REFERENCES

1. Stoddart JF. Molecular machines. *Acc Chem Res* 2001, 34:410–411.
2. Coskun A, Banaszak M, Astumian RD, Stoddart JF, Grzybowski BA. Great expectations: can artificial molecular machines deliver on their promise? *Chem Soc Rev* 2012, 41:19–30.
3. Michl J, Sykes ECH. Molecular rotors and motors: recent advances and future challenges. *ACS Nano* 2009, 3:1042–1048.
4. Browne WR, Feringa BL. Making molecular machines work. *Nat Nanotechnol* 2006, 1:25–35.
5. Kay ER, Leigh DA, Zerbetto F. Synthetic molecular motors and mechanical machines. *Angew Chem Int Ed* 2007, 46:72–191.
6. Balzani V, Credi A, Venturi M. Light powered molecular machines. *Chem Soc Rev* 2009, 38:1542–1550.
7. Kelly TR, De Silva H, Silva RA. Unidirectional rotary motion in a molecular system. *Nature* 1999, 401:150–152.
8. Fletcher SP, Dumur F, Pollard MM, Feringa BL. A reversible, unidirectional molecular rotary motor driven by chemical energy. *Science* 2005, 310:80–82.
9. Kudernac T, Raungsupapichat N, Parschau M, Macia B, Katsonis N, Harutyunyan SR, Ernst K-H, Feringa BL. Electrically driven directional motion of a four-wheeled molecule on a metal surface. *Nature* 2011, 479:208–211.
10. Tierney HL, Murphy CJ, Jewell AD, Baber AE, Iski EV, Khodaverdian HY, McGuire AF, Klebanov N, Sykes ECH. Experimental demonstration of a single-molecule electric motor. *Nat Nanotechnol* 2011, 6:625–629.
11. Koumura N, Zijlstra RWJ, Van Delden RA, Harada N, Feringa BL. Light-driven monodirectional molecular rotor. *Nature* 1999, 401:152–155.
12. Koumura N, Geertsema EM, Van Gelder MB, Meetsma A, Feringa BL. Second generation light-driven molecular motors. Unidirectional rotation controlled by a single stereogenic center with near-perfect photoequilibria and acceleration of the speed of rotation by structural modification. *J Am Chem Soc* 2002, 124:5037–5051.
13. Pollard MM, Meetsma A, Feringa BL. A redesign of light-driven rotary molecular motors. *Org Biomol Chem* 2008, 6:507–512.
14. Credi A. Artificial molecular motors powered by light. *Aust J Chem* 2006, 59:157–169.
15. London G, Carroll GT, Fernandez Landaluce T, Pollard MM, Rudolf P, Feringa BL. Light-driven altitudinal molecular motors on surfaces. *Chem Commun* 2009:1712–1714.
16. Chiang P-T, Mielke J, Godoy J, Guerrero JM, Alemany LB, Villagómez CJ, Saywell A, Grill L, Tour JM. Toward a light-driven motorized nanocar: synthesis and initial imaging of single molecules. *ACS Nano* 2012, 6:592–597.
17. Morin J-F, Shirai Y, Tour JM. En route to a motorized nanocar. *Org Lett* 2006, 8:1713–1716.
18. Fernández Landaluce T, London G, Pollard MM, Rudolf P, Feringa BL. Rotary molecular motors: a large increase in speed through a small change in design. *J Org Chem* 2010, 75:5323–5325.
19. Knowles P, Schütz M, Werner H-J. Ab initio methods for electron correlation in molecules. In: Grotendorst J, ed. *Modern Methods and Algorithms of Quantum Chemistry*. Jülich, Germany: John von Neumann Institute for Computing, NIC Series; 2000, 3:97–179.
20. Roca-Sanjuán D, Aquilante F, Lindh R. Multiconfiguration second-order perturbation theory approach to strong electron correlation in chemistry and photochemistry. *WIREs Comput Mol Sci* 2012, 2:585–603.
21. Grimm S, Bräuchle C, Frank I. Light-driven unidirectional rotation in a molecule: ROKS simulation. *ChemPhysChem* 2005, 6:1943–1947.
22. Kazaryan A, Filatov M. Density functional study of the ground and excited state potential energy surfaces of a light-driven rotary molecular motor

(3R,3′R)-(P,P)-trans-1,1′,2,2′,3,3′,4,4′-octahydro-3,3′-dimethyl-4,4′-biphenanthrylidene. *J Phys Chem A* 2009, 113:11630–11634.

23. Kazaryan A, Kistemaker JCM, Schäfer LV, Browne WR, Feringa BL, Filatov M. Understanding the dynamics behind the photoisomerization of a light-driven fluorene molecular rotary motor. *J Phys Chem A* 2010, 114:5058–5067.
24. Kazaryan A, Lan Zh, Schäfer LV, Thiel W, Filatov M. Surface hopping excited-state dynamics study of the photoisomerization of a light-driven fluorene molecular rotary motor. *J Chem Theory Comput* 2011, 7:2189–2199.
25. Conyard J, Addison K, Heisler IA, Cnossen A, Browne WR, Feringa BL, Meech SR. Ultrafast dynamics in the power stroke of a molecular rotary motor. *Nat Chem* 2012, 4:547–551.
26. Pollard MM, Wesenhagen PV, Pijper D, Feringa BL. On the effect of donor and acceptor substituents on the behaviour of light-driven rotary molecular motors. *Org Biomol Chem* 2008, 6:1605–1612.
27. Levine BG, Martinez TJ. Isomerization through conical intersections. *Annu Rev Phys Chem* 2007, 58:613–634.
28. Zewail AH. Femtochemistry: atomic-scale dynamics of the chemical bond. *J Phys Chem A* 2000, 104:5660–5694, and references cited therein.
29. Yarkony DR. Diabolical conical intersections. *Rev Mod Phys* 1996, 68:985–1013.
30. Bernardi F, Olivucci M, Robb MA. Potential energy surface crossings in organic photochemistry. *Chem Soc Rev* 1996, 25:321–328.
31. Levine BG, Coe JD, Martinez TJ. Optimizing conical intersections without derivative coupling vectors: application to multistate multireference second-order perturbation theory (MS-CASPT2). *J Phys Chem B* 2008, 112:405–413.
32. Virshup AM, Chen J, Martínez TJ. Nonlinear dimensionality reduction for nonadiabatic dynamics: the influence of conical intersection topography on population transfer rates. *J Chem Phys* 2012, 137:22A519.
33. Born M, Oppenheimer R. Zur Quantentheorie der Molekeln. *Ann Phys* 1927, 84:457–484.
34. Robb MA, Bernardi F, Olivucci M. Conical intersections as a mechanistic feature of organic photochemistry. *Pure Appl Chem* 1995, 67:783–789.
35. Von Neumann J, Wigner EP. Uber das Verhalten von Eigenwerten bei adiabatischen Prozessen. *Z Physik* 1929, 30:467–470.
36. Teller E. The crossing of potential energy surfaces. *J Phys Chem* 1937, 41:109–116.
37. Longuet-Higgins HC. The intersection of potential energy surfaces in polyatomic molecules. *Proc R Soc Lond Ser A* 1975, 344:147–156.
38. Manaa MR, Yarkony DR. On the intersection of two potential energy surfaces of the same symmetry. Systematic characterization using a Lagrange multiplier constrained procedure. *J Chem Phys* 1993, 99:5251–5256.
39. Bearpark MJ, Robb MA, Schlegel HB. A direct method for the location of the lowest energy point on a potential surface crossing. *Chem Phys Lett* 1994, 223:269–274.
40. Ben-Nun M, Martinez TJ. Photo-dynamics of ethylene: ab initio studies of conical intersections. *Chem Phys* 2000, 259:237–248.
41. Quenneville J, Martinez TJ. Ab initio study of *cis–trans* photo-isomerization in stilbene and ethylene. *J Phys Chem A* 2003, 107:829–837.
42. Garavelli M, Celani P, Bernardi F, Robb MA, Olivucci M. The $C_5H_6NH_2^+$ protonated Schiff base: an ab initio minimal model for retinal photo-isomerization. *J Am Chem Soc* 1997, 119:6891–6901.
43. Fukui K. Formulation of the reaction coordinate. *J Phys Chem* 1970, 74:4161–4163.
44. Coe JD, Ong MT, Levine BG, Martinez TJ. On the extent and connectivity of conical intersection seams and the effects of three-state intersections. *J Phys Chem A* 2008, 112:12559–12567.
45. Yarkony DR. Nuclear dynamics near conical intersections in the adiabatic representation: I. The effects of local topography on interstate transitions. *J Chem Phys* 2001, 114:2601–2613.
46. Car R, Parrinello M. Unified approach for molecular-dynamics and density-functional theory. *Phys Rev Lett* 1985, 55:2471–2474.
47. Sawada S-I, Nitzan A, Metiu H. Mean-trajectory approximation for charge- and energy-transfer processes at surfaces. *Phys Rev B* 1985, 32:851–867.
48. Li XS, Tully JC, Schlegel HB, Frisch MJ. Ab initio Ehrenfest dynamics. *J Chem Phys* 2005, 123:084106.
49. Tully JC, Preston RK. Trajectory surface hopping approach to non-adiabatic molecular collisions: the reaction of H^+ with D_2. *J Chem Phys* 1971, 55:562–572.
50. Tully JC. Molecular dynamics with electronic transitions. *J Chem Phys* 1990, 93:1061–1071.
51. Barbatti M. Nonadiabatic dynamics with trajectory surface hopping method. *WIREs Comput Mol Sci* 2011, 1:620–633.
52. Parandekar PV, Tully JC. Detailed balance in ehrenfest mixed quantum-classical dynamics. *J Chem Theory Comput* 2006, 2:229–235.
53. Meyer HD, Manthe U, Cederbaum LS. The multi-configurational time-dependent Hartree approach. *Chem Phys Lett* 1990, 165:73–78.
54. Martinez TJ, Ben-Nun M, Levine RD. Multi-electronic-state molecular dynamics: a wave function approach with applications. *J Phys Chem* 1996, 100:7884–7895.

55. Ben-Nun M, Quenneville J, Martınez TJ. Ab initio multiple spawning: photochemistry from first principles molecular dynamics. *J Phys Chem A* 2000, 104:5161–5175.
56. Celani P, Werner H-J. Analytical energy gradients for internally contracted second-order multireference perturbation theory. *J Chem Phys* 2003, 119:5044–5057.
57. Shiozaki T, Györffy W, Celani P, Werner H-J. Extended multi-state complete active space second-order perturbation theory: energy and nuclear gradients. *J Chem Phys* 2011, 135:081106.
58. Shepard R, Lischka H, Szalay PG, Kovar T, Ernzerhof M. A general multi-reference configuration interaction gradient program. *J Chem Phys* 1992, 96:2085–2098.
59. Lischka H, Dallos M, Shepard R. Analytic MRCI gradient for excited states: formalism and application to the n-π^* valence- and n-(3s,3p) Rydberg states of formaldehyde. *Mol Phys* 2002, 100:1647–1658.
60. Burke K. Perspective on density functional theory. *J Chem Phys* 2012, 136:150901, and references cited therein.
61. Cremer D. Density functional theory: coverage of dynamic and non-dynamic electron correlation effects. *Mol Phys* 2001, 99:1899–1940.
62. See, Burke K, Werschnik J, Gross EKU. Time-dependent density functional theory: past, present, and future. *J Chem Phys* 2005, 123:062206, and references cited therein.
63. Kazaryan A, Heuver J, Filatov M. Excitation energies from spin-restricted ensemble-referenced Kohn–Sham method: a state-average approach. *J Phys Chem A* 2008, 112:12980–12988.
64. Lieb EH. Density functionals for coulomb systems. *Int J Quantum Chem* 1983, 24:243–277.
65. Filatov M, Shaik S. Spin-restricted density functional approach to the open-shell problem. *Chem Phys Lett* 1998, 288:689–697.
66. Filatov M, Shaik S. A spin-restricted ensemble-referenced Kohn–Sham method and its application to diradicaloid situations. *Chem Phys Lett* 1999, 304:429–437.
67. Frank I, Hutter J, Marx D, Parinello M. Molecular dynamics in low-spin excited states. *J Chem Phys* 1998, 108:4060–4069.
68. Gaudoin R, Burke K. Lack of Hohenberg–Kohn theorem for excited states. *Phys Rev Lett* 2004, 93:173001.
69. Schautz F, Buda F, Filippi C. Excitations in photoactive molecules from quantum Monte Carlo. *J Chem Phys* 2004, 121:5836–5844.
70. Weber W, Thiel W. Orthogonalization corrections for semi-empirical methods. *Theor Chem Acc* 2000, 103:495–506.
71. Koslowski A, Beck ME, Thiel W. Implementation of a general multi-reference configuration interaction procedure with analytic gradients in a semi-empirical context using the graphical unitary group approach. *J Comput Chem* 2003, 24:714–726.
72. Thiel W. *MNDO program, version 6.1*. Mülheim an der Ruhr, Germany: Max-Planck-Institut für Kohlenforschung; 2007.
73. Barbatti M, Lan Zh, Crespo-Otero R, Szymczak JJ, Lischka H, Thiel W. Critical appraisal of excited state nonadiabatic dynamics simulationsof 9H-adenine. *J Chem Phys* 2012, 137:22A503.
74. Augulis R, Klok M, Feringa BL, van Loosdrecht PHM. Light-driven rotary molecular motors: an ultrafast optical study. *Phys Stat Sol C* 2009, 6:181–184.

